

Enhanced Charge Storage of Nanometric  $\zeta$ -V<sub>2</sub>O<sub>5</sub> in Mg Electrolytes

*Ian D. Johnson<sup>1,2,3</sup>, Gene Nolis<sup>3,4,5</sup>, Liang Yin<sup>3,6</sup>, Hyun Deog Yoo<sup>3,4,7</sup>, Prakash Parajuli<sup>3,8</sup>, Arijita Mukherjee<sup>3,8</sup>, Justin L. Andrews<sup>9</sup>, Mario Lopez<sup>3,4</sup>, Robert F. Klie<sup>3,8</sup>, Sarbajit Banerjee<sup>9</sup>, Brian J. Ingram<sup>2,3</sup>, Saul Lapidus<sup>3,6</sup>, Jordi Cabana<sup>3,4\*</sup>, Jawwad A. Darr<sup>1\*</sup>*

<sup>1</sup> Department of Chemistry, University College London, London, UK.

<sup>2</sup> Chemical Sciences and Engineering Division, Argonne National Laboratory, Lemont, Illinois 60439, United States

<sup>3</sup> Joint Center for Energy Storage Research, Argonne National Laboratory, Lemont, IL 60439, USA.

<sup>4</sup> Department of Chemistry, University of Illinois at Chicago, Chicago, IL 60607, USA.

<sup>5</sup> Electrochemical Energy Storage, CIC EnergiGUNE, Vitoria-Gasteiz 01510 Spain.

<sup>6</sup> X-ray Science Division, Argonne National Laboratory, Lemont, Illinois 60439, United States

<sup>7</sup> Department of Chemistry and Chemical Institute for Functional Materials, Pusan National University, Busan 46241, Republic of Korea.

<sup>8</sup> Department of Physics, University of Illinois at Chicago, Chicago, IL 60607, USA

<sup>9</sup> Department of Chemistry, Texas A&M University, College Station, TX 77843, USA

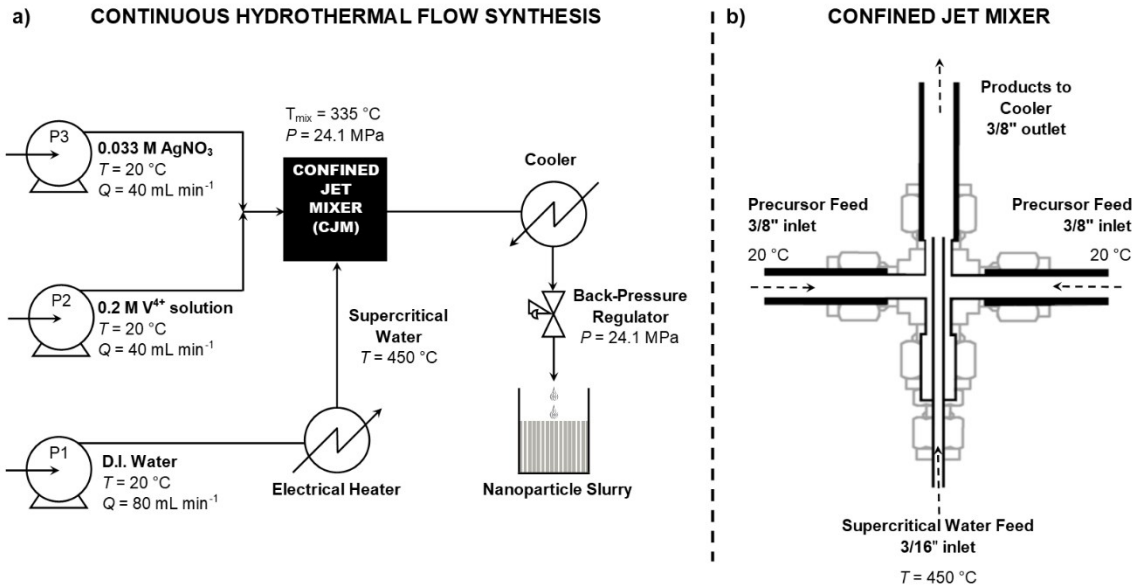


Figure S1. a) A schematic of the Continuous Hydrothermal Flow Synthesis (CHFS) apparatus; b) a schematic of the Confined Jet Mixer (CJM).

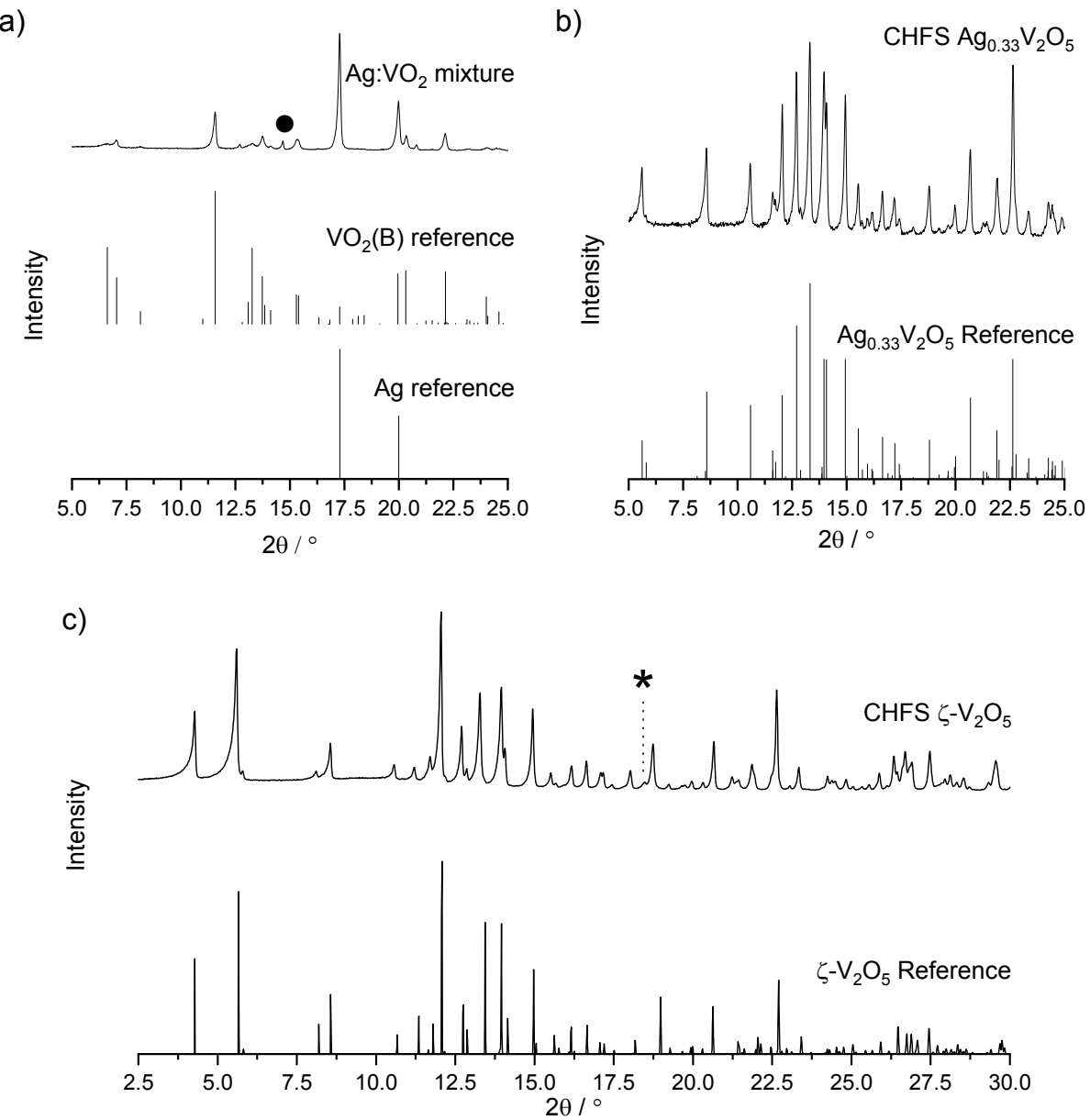


Figure S2. XRD patterns (Mo-K $\alpha$  radiation) of a) the direct product of the CHFS process, which appeared to be a mixture of VO<sub>2</sub>(B) and Ag (PDFs 00-081-2392 and 01-089-3722 respectively, although an additional diffraction peak was present as indicated with ● symbols), b) the annealed product CHFS Ag<sub>0.33</sub>V<sub>2</sub>O<sub>5</sub>, which matched the Ag<sub>0.33</sub>V<sub>2</sub>O<sub>5</sub> reference pattern (PDF 01-082-1177), and c) the product of acid leaching, Nano  $\zeta$ -V<sub>2</sub>O<sub>5</sub>, which matched a simulated diffraction pattern from parameters described in reference 30, although an additional feature was observed at 18.5° 2θ from the collimator, and is marked with a \* symbol.

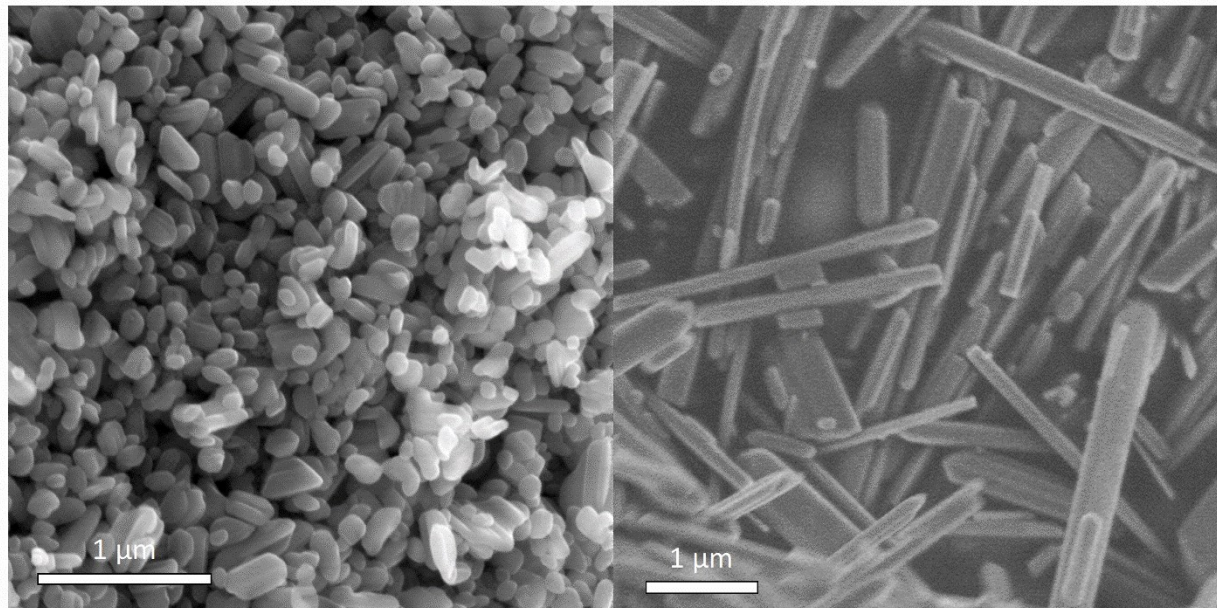


Figure S3. a) SEM image of the Nano  $\zeta$ - $\text{V}_2\text{O}_5$  sample, displaying sub-100 nm semi-spherical crystallites with a small population of faceted rods up to 500 nm in length. b) SEM image of the Bulk  $\zeta$ - $\text{V}_2\text{O}_5$  sample, displaying rod-morphology, with lengths in the  $\mu\text{m}$ -scale and an average width of  $\sim 150$  nm.

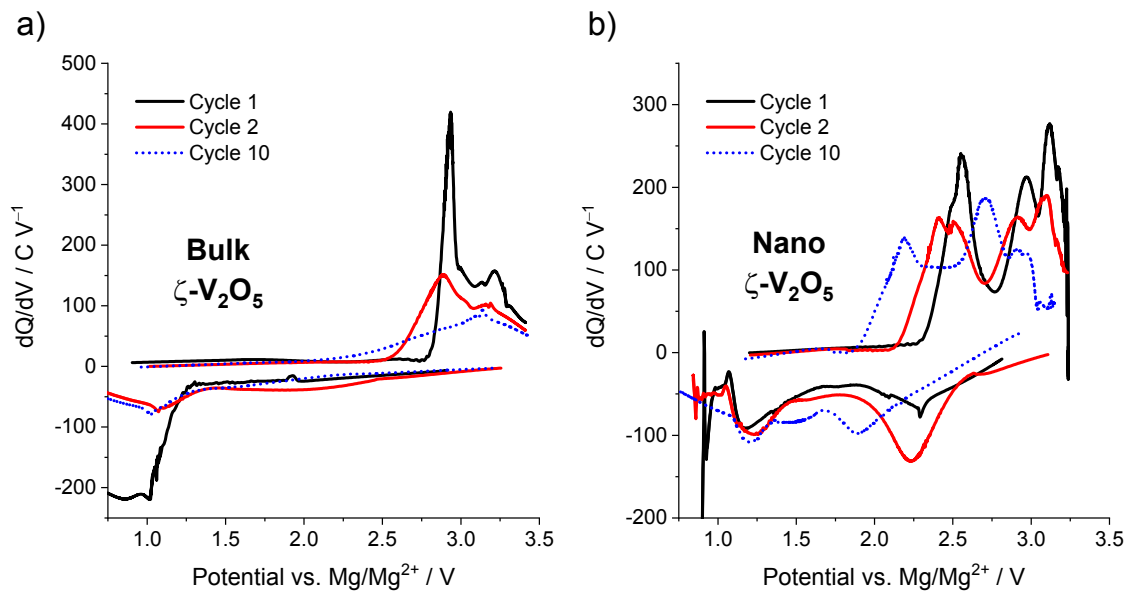


Figure S4.  $dQ/dV$  profiles of the first, second, and tenth cycles of a) Bulk  $\zeta$ - $\text{V}_2\text{O}_5$  and b) Nano  $\zeta$ - $\text{V}_2\text{O}_5$ .

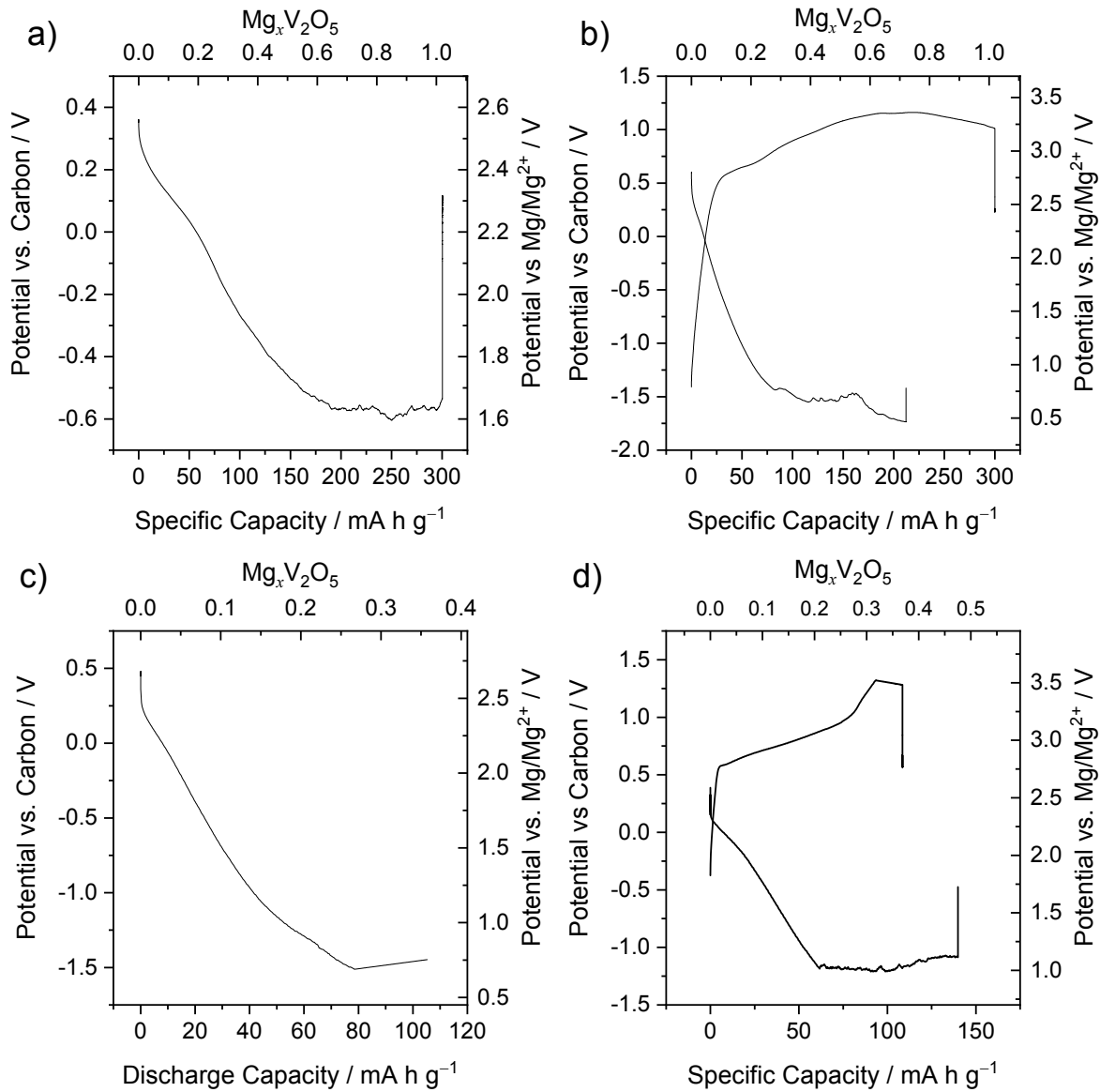


Figure S5. Discharge curves for the a) discharged and b) charged electrodes used for the XAS analysis. Discharged curves for the c) discharged and d) charged electrodes used for the XRD, EDS, and HAADF-STEM analysis.

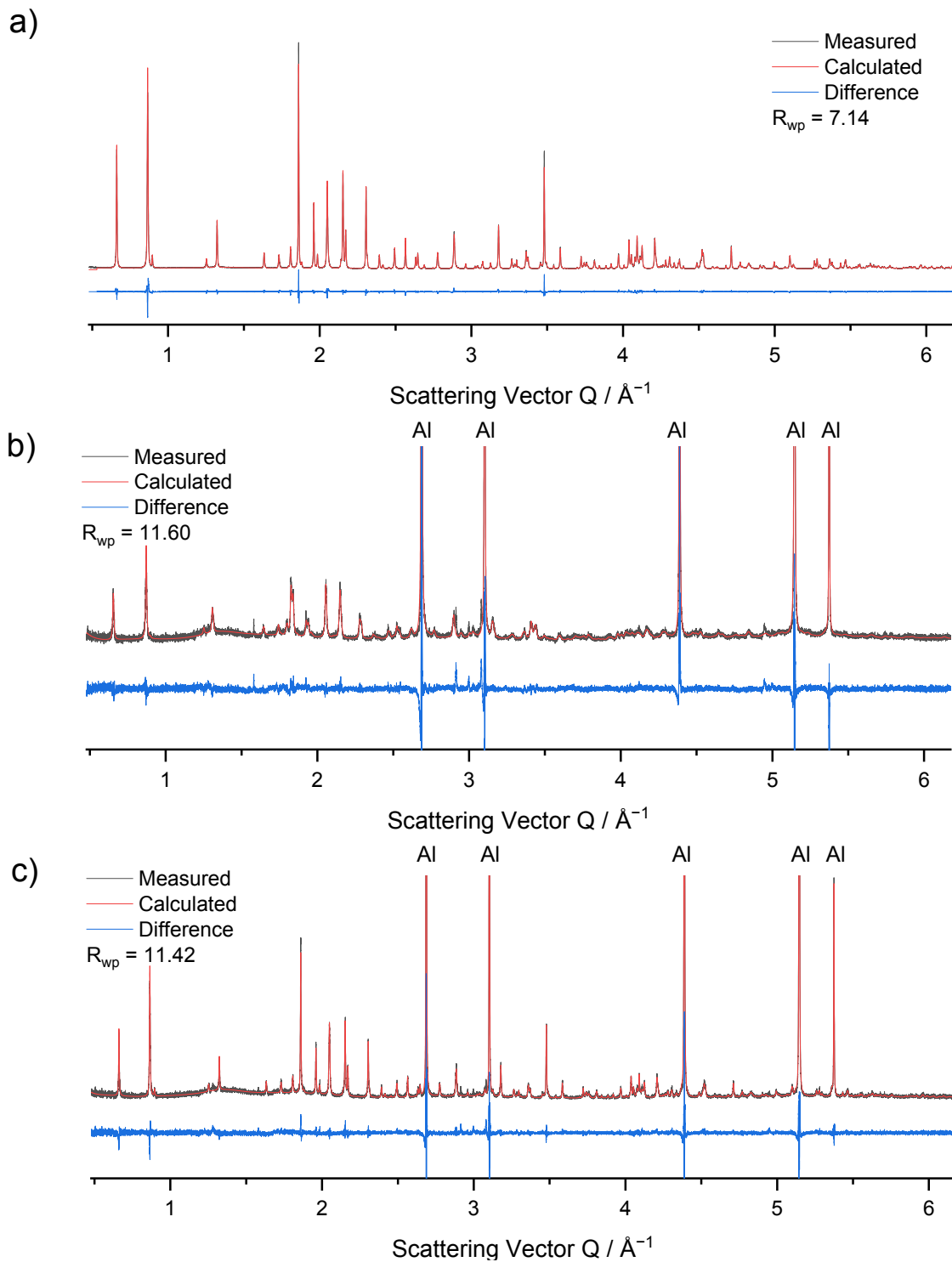


Figure S6. Rietveld refinement plots of the a) Pristine, b) Discharged and c) Charged electrodes, with Al electrode substrate diffraction peaks indicated within the plots. The diffraction angle was normalized to scattering vector  $Q$  to ensure consistent comparison between the diffraction patterns, as the wavelength  $\lambda$  varied slightly between measurements.

Table S1. Unit cell parameters and atomic coordinates for the pristine Nano  $\zeta$ -V<sub>2</sub>O<sub>5</sub> sample.

a = 15.40841(4) Å, b = 3.610815(6) Å, c = 10.078048(20) Å, $\beta$ = 109.56366(17) $^\circ$ , V = 528.342(2) Å <sup>3</sup> Space Group C12/m1, R <sub>wp</sub> = 7.14, $\chi^2$ = 1.23					
Atom	x	y	z	Occupancy	B <sub>eq</sub>
V1	0.33790(3)	0	0.10134(4)	1	0.378(8)
V2	0.11646(3)	0	0.11866(4)	1	0.380(8)
V3	0.28803(3)	0	0.40974(5)	1	0.414(9)
O1	0	0	0	1	0.52(4)
O2	0.10629(11)	0	0.27069(15)	1	0.76(3)
O3	0.13377(11)	0.5	0.07729(14)	1	0.18(3)
O4	0.26295(10)	0	0.22174(15)	1	0.31(3)
O5	0.43610(10)	0	0.21925(15)	1	0.90(3)
O6	0.31506(10)	0.5	0.05500(14)	1	0.27(3)
O7	0.39754(11)	0	0.47083(16)	1	1.10(3)
O8	0.25742(10)	0.5	0.42610(15)	1	0.45(3)
Na	0.00128(17)	0	0.4067(2)	0.4430(18)	1.89(6)

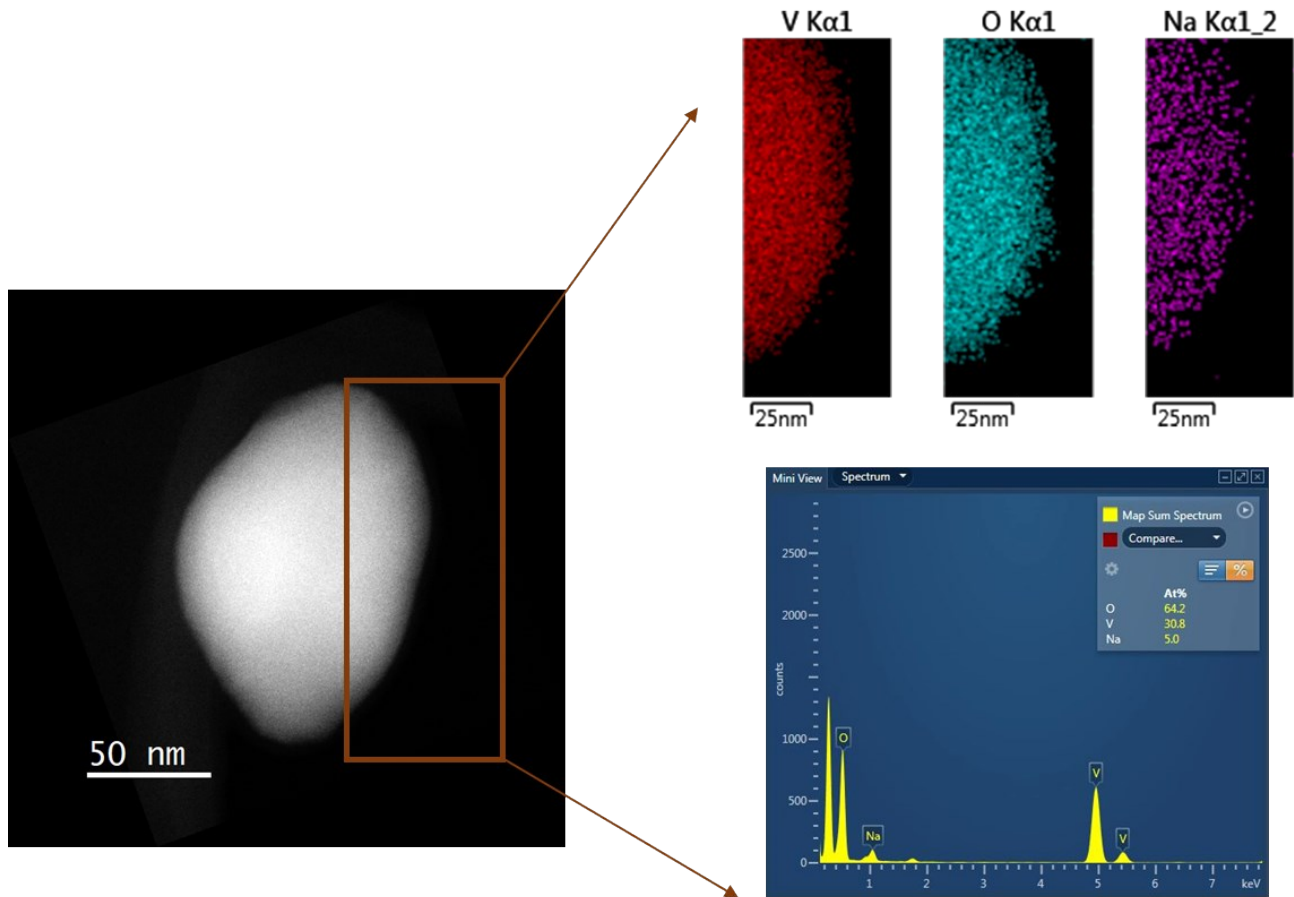


Figure S7. EDS analysis of a particle within the Pristine electrode.

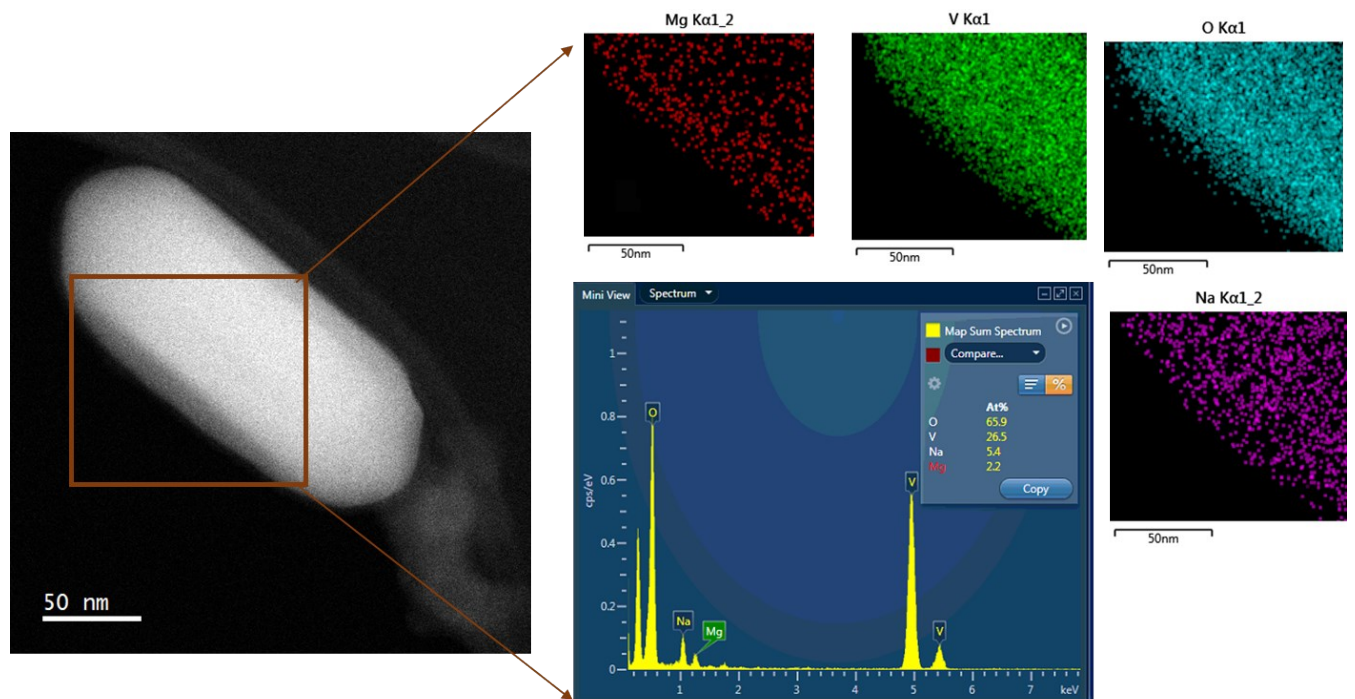


Figure S8. EDS analysis of a particle within the Discharged electrode.

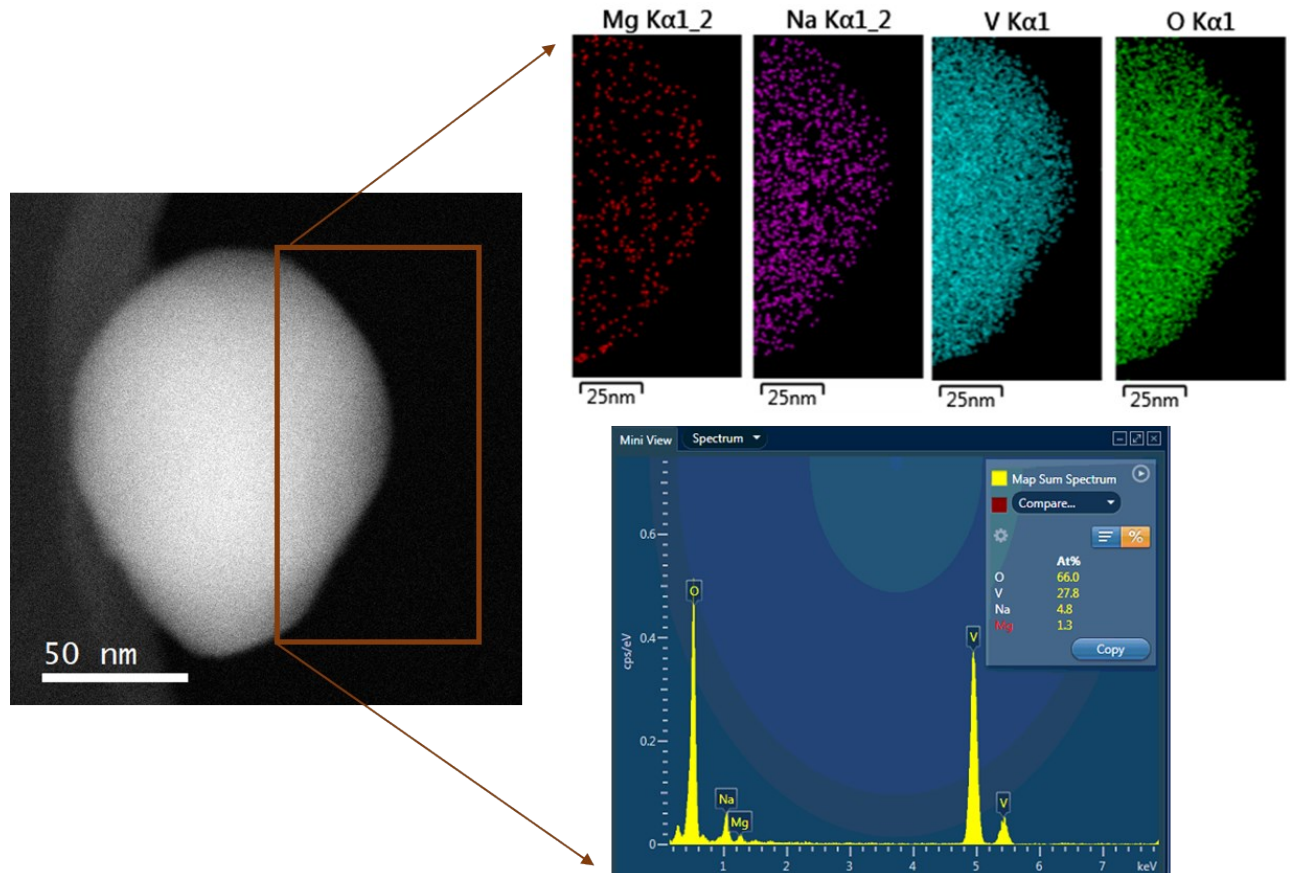


Figure S9. EDS analysis of a particle within the Charged electrode.

Table S2. Elemental composition found by EDS characterization.

Material	Na content	Mg content	V content <sup>a</sup>
Pristine <sup>b</sup>	0.31(5)	0	2
Discharged <sup>b</sup>	0.45(14)	0.18(11)	2
Charged <sup>b</sup>	0.40(13)	0.09(5)	2

<sup>a</sup> The atomic content has been normalized such that V = 2 in all cases, allowing facile stoichiometric comparison between the pristine, discharged and charged states. <sup>b</sup> Elemental composition averaged over a minimum of 5 particles.

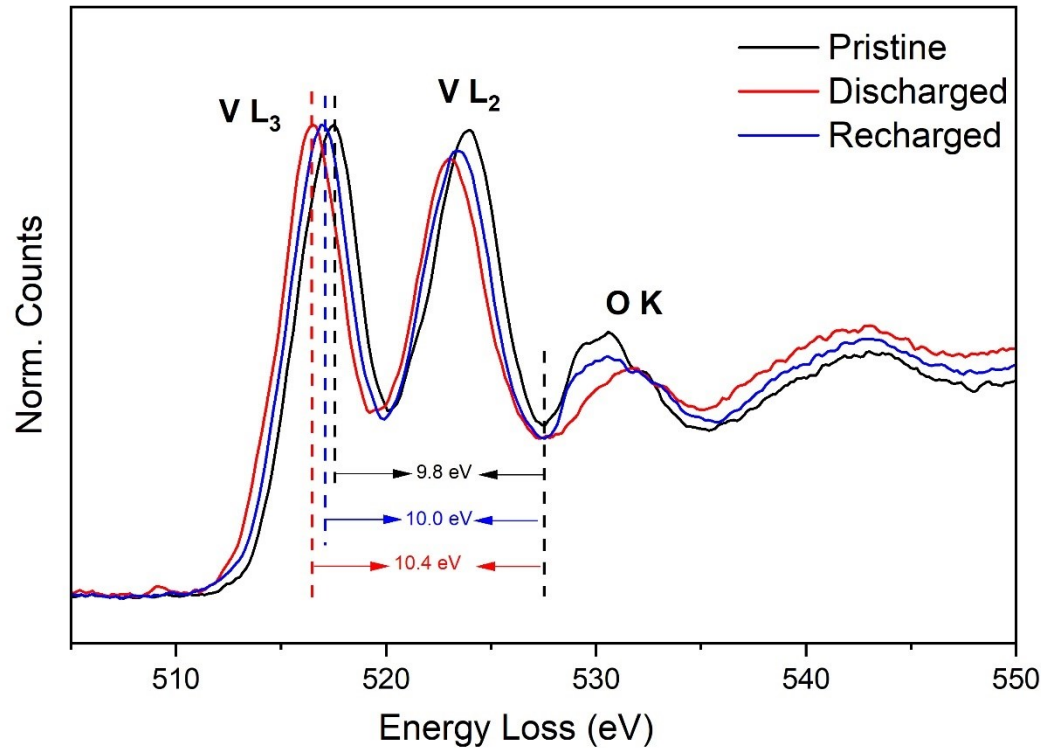


Figure S10. a) Electron Energy Loss Spectroscopy (EELS) spectra of the pristine, discharged and charged electrodes of Nano  $\zeta$ -V<sub>2</sub>O<sub>5</sub>.